

Testing MOG, Non-Local Gravity and MOND with rotation curves of dwarf galaxies

M.H. Zhooldideh Haghighi ^{*}, S. Rahvar [†]

Department of Physics, Sharif University of Technology, P.O. Box 11155-9161, Tehran, Iran

28 February 2017

ABSTRACT

Modified Gravity (MOG) and Non-Local Gravity (NLG) are two alternative theories to General Relativity. They are able to explain the rotation curves of spiral galaxies and clusters of galaxies without including dark matter (Moffat & Rahvar 2013, 2014; Rahvar & Mashhoon 2014). In the weak-field approximation these two theories have similar forms, with an effective gravitational potential that has two components: (i) Newtonian gravity with the gravitational constant enhanced by a factor $(1 + \alpha)$ and (ii) a Yukawa type potential that produces a repulsive force with length scale $1/\mu$. In this work we compare the rotation curves of dwarf galaxies in the LITTLE THINGS catalog with predictions of MOG, NLG and Modified Newtonian Dynamics (MOND). We find that the universal parameters of these theories, can fit the rotation curve of dwarf galaxies with a larger stellar mass to the light ratio compared to the nearby stars in the Milky Way galaxy. Future direct observations of mass function of stars in the dwarf galaxies can examine different modified gravity models.

1 INTRODUCTION

At the scales of galaxies and clusters of galaxies, observations show a systemic discrepancy between dynamical mass models and the mass distributions inferred from the luminous matter (Zwicky 1937; Rubin et al. 1965, 1970). One proposal for resolving this discrepancy is dark matter—so-called missing mass of the Universe. Cosmological dark matter is a fluid composed of massive particles that interact gravitationally with each other, with the possibility of very weak non-gravitational interaction with themselves and with ordinary (baryonic) matter. The most accurate and acceptable model of dark matter is Λ CDM which by having six parameters explains CMB data (Spergel 2015), large scale structure of the universe (Blumenthal et al. 1984) and Baryonic Acoustic Oscillations (Eisenstein et al. 2005). It should be noted that it is hard for any alternative theory to explain such a wide range of observations that Λ CDM do. While dark matter is successful in interpretation of observations, no explicit signal of dark matter particle interaction with the ordinary matter has yet been found (Moore et al. 2001; Gaitskell 2004; Angloher et al. 2012; Akerib et al. 2014). Recent observations of 153 galaxies with different morphology, mass, size and gas fraction shows that there is a strong correlation between observed radial acceleration and acceleration results from the baryonic matter (McGaugh et al. 2016), which maybe suggests new dynamical laws rather than dark matter. Moreover in the gravitational lensing, Sanders & Land (2008) showed that mass derived from the lensing within the Einstein ring has linear correlation with the surface brightness.

An alternative approach to interpret the dynamics of large structures is to analyze observations using a modified

law of gravity, with no dark matter. One well known model is Modified Newtonian Dynamics (MOND), which changes the Newtonian dynamics at small accelerations in a way that produces flat rotation curves for spiral galaxies (Milgrom 1983). MOND was extended to a relativistic theory by Bekenstein (2004). Some challenges facing MOND and other modified gravity theories are to explain the gravitational lensing of systems like the bullet cluster (Markevitch et al. 2004) and the large scale structure formation in the Universe without using dark matter. Although it seems that MOND can not be made consistent with the detailed shape of the CMB and matter power spectra, there are some works on hybrid models which include both DM and MOND phenomena (Bruneton et al. 2009; Khoury 2015) and explain both the dynamic of galaxies and cosmological observations.

Another modification to the gravity is done by Hehl & Mashhoon (2009) where they introduced Non-Local Gravity (NLG), with a modified gravitational acceleration, to solve the missing mass problem. NLG extends non-local special relativity to the accelerating frames. In the weak-field, non-relativistic limit of NLG, the effective gravitational potential of a point mass adds to a Newton-like potential a new term that gives a repulsive, Yukawa-like force (Hehl & Mashhoon 2009). Predictions of this theory have been compared with the rotation curves of spiral galaxies and the temperature profiles of hot gas for clusters of galaxies in the Chandra database. With the fixed values for the parameters of NLG, the dynamics of spiral galaxies and clusters of galaxies are consistent with the baryonic distribution of matter in these systems, with no need for dark matter (Rahvar & Mashhoon 2014).

Modified Gravity (MOG) theory—a covariant extension

arXiv:1609.07851v2 [astro-ph.GA] 25 Feb 2017

of General Relativity—also avoids the need for dark matter (Moffat 2006). In MOG, gravity is described by the tensor metric field in combination with new scalar and vector fields. An important feature is that each particle has a fifth force charge, proportional to its inertial mass, through which it couples to the massive vector field. Similar to the Lorentz acceleration of charged particles in electrodynamics, test particles in MOG deviate from geodesics due to coupling of their fifth force charge with the vector field. In the weak-field approximation a modified Poisson equation is obtained, which for a point-like mass has a Yukawa repulsive term in addition to a conventional Newtonian potential. Comparison with the dynamics of spiral galaxies in the THINGS catalog results in universal values for the parameters of this model, with reasonable fits to the rotation curves of galaxies and clusters of galaxies (Moffat & Rahvar 2013, 2014). For all the modified gravity models, the crucial observational tests would be predicting (i) the angular power spectrum of CMB (ii) the power spectrum of large scale structures and the other consequences of structure formation as the Baryonic acoustic oscillations.

Although NLG and MOG have completely different physical axioms, they have almost same behaviour in the weak-field approximation limit. To test the universality of parameters of modified gravity models at intermediate scales, we use the dynamical and luminosity data of dwarf galaxies in the LITTLE THINGS catalog and interpret them in the effective potentials of MOG, NLG, and MOND. The observational data in the LITTLE THINGS catalog are the density distributions of stars and gas of each galaxy as well as the dynamics in form of galaxy rotation curves.

In Section 2, we review three alternative theories of gravity of (i) Modified Gravity (MOG) and its weak field approximation (ii) Non-Local Gravity (NLG) and the corresponding weak field approximation (iii) and Modified Newtonian Dynamics (MOND). In Section 3, we introduce the LITTLE THINGS catalog and apply the results of weak field approximation of alternative models of gravity to the dwarf galaxies. We determine the best-fitting values for the stellar mass to light ratio for our three model. The conclusion is given in Section 4 where we discuss the universality of parameters of modified gravity theories and a larger stellar mass to light ratio for dwarf galaxies which can be used to examine the modified gravity models with the future direct observations of stellar mass function in these galaxies.

2 ALTERNATIVE THEORIES TO DARK MATTER

One of the important questions in cosmology is how to interpret the dynamics of structures such as clusters of galaxies and spiral galaxies, for which the observed baryonic matter is not enough (Zwicky 1937; Rubin et al. 1965, 1970). An alternative to assuming the existence of dark matter is to modify the theory of gravity in a way that can explain the observations with only baryonic matter. In this section we introduce three models for the modification of gravity law. Modified Gravity (MOG) which was introduced by Moffat (2006) and the weak field approximation detailed in Moffat & Rahvar (2013). Non-Local Gravity (NLG), where the Einstein equations in the teleparallel form are similar to the

Maxwell equations, hence these equations can be written in a non-local way (Hehl & Mashhoon 2009). Modified Newtonian Dynamics (MOND) modifies Newton’s law of gravity for small accelerations (Milgrom 1983).

2.1 Field equations in MOG

We use the metric signature convention $(-, +, +, +)$. The general form of action for MOG, which is also called Scalar-Tensor-Vector-Gravity (STVG), is given by (Moffat 2006; Moffat & Toth 2009):

$$S = S_G + S_\phi + S_S + S_M, \quad (1)$$

where S_G is the standard Einstein action:

$$S_G = \frac{1}{16\pi} \int \frac{1}{G} (R + 2\Lambda) \sqrt{-g} d^4x, \quad (2)$$

and S_ϕ and S_S are the actions for the massive vector and scalar fields and take the forms:

$$S_\phi = \frac{1}{4\pi} \int \omega \left[\frac{1}{4} B^{\mu\nu} B_{\mu\nu} - \frac{1}{2} \mu^2 \phi_\mu \phi^\mu + V_\phi(\phi_\mu \phi^\mu) \right] \sqrt{-g} d^4x, \quad (3)$$

and

$$S_S = \int \frac{1}{G} \left[\frac{1}{2} g^{\alpha\beta} (G^{-2} \nabla_\alpha G \nabla_\beta G + \mu^{-2} \nabla_\alpha \mu \nabla_\beta \mu) - G^{-2} V_G(G) - \mu^{-2} V_\mu(\mu) \right] \sqrt{-g} d^4x. \quad (4)$$

Here ∇_ν is the covariant derivative with respect to the metric $g_{\mu\nu}$; the Faraday tensor of the vector field is defined by $B_{\mu\nu} = \partial_\mu \phi_\nu - \partial_\nu \phi_\mu$; ω is a dimensionless coupling constant; G is a scalar field representing the gravitational coupling strength; and μ is a scalar field corresponding to the mass of the vector field. Also $V_\phi(\phi_\mu \phi^\mu)$, $V_G(G)$ and $V_\mu(\mu)$ are the self-interaction potentials associated with the vector field and the scalar fields, respectively. In our analysis we consider a simplified version of this action, setting all the potentials to zero and making ω and μ constant parameters.

The action for pressureless dust can be written as

$$S_M = \int (\rho \sqrt{-u^\mu u_\mu} - \omega J^\mu \phi_\mu) \sqrt{-g} dx^4, \quad (5)$$

For a point mass particle we substitute $\rho(x) = m \delta^3(x)$. Varying this action results in the geodesic equation:

$$\frac{du^\mu}{d\tau} + \Gamma_{\alpha\beta}^\mu u^\alpha u^\beta = \omega \kappa B^\mu{}_\alpha u^\alpha. \quad (6)$$

We note that m has cancelled out. The acceleration term on the right hand side of this equation causes deviation from geodesics similar to the Lorentz acceleration in the electrodynamics—the only difference is that the vector field in this action is massive, and hence provides a short range interaction.

At astrophysical scales we use the non-relativistic, weak field approximation of MOG. This has been shown to yield good agreement with the dynamics of spiral galaxies and clusters of galaxies (Moffat & Rahvar 2013). Here, we review the same procedure by expanding fields around the Minkowski space-time in the action as follows:

$$g_{\mu\nu} = \eta_{\mu\nu} + h_{\mu\nu}, \quad (7)$$

where $\eta_{\mu\nu}$ is the Minkowski metric. For the vector field, we write

$$\phi_\mu = \phi_{\mu(0)} + \phi_{\mu(1)}, \quad (8)$$

where $\phi_{\mu(0)}$ is the zeroth order and $\phi_{\mu(1)}$ is the first order perturbation of the vector field. For Minkowski space-time, we set $\phi_{\mu(0)}$ equal to zero since in the absence of matter there is no gravity source for the vector field ϕ_μ . We also perturb the energy-momentum tensor about the Minkowski background:

$$T_{\mu\nu} = T_{\mu\nu(0)} + T_{\mu\nu(1)}, \quad (9)$$

where $T_{\mu\nu(0)}$ is zero.

By substituting the perturbed forms in the action, varying the action with respect to the metric, and ignoring the higher orders of perturbation, we get the field equation

$$R_{\mu\nu(1)} - \frac{1}{2}R_{(1)}\eta_{\mu\nu} = 8\pi G_0 T_{\mu\nu(1)}^{(M)} + 8\pi G_0 T_{\mu\nu(1)}^{(\phi)}, \quad (10)$$

where $T_{\mu\nu(1)}^{(M)}$ represents the energy-momentum tensor of matter, and $T_{\mu\nu(1)}^{(\phi)}$ is the energy-momentum tensor of the vector field given by

$$\begin{aligned} T_{\mu\nu}^{(\phi)} &= -\frac{\omega}{4\pi}(B_\mu^\alpha B_{\nu\alpha} - \frac{1}{4}g_{\mu\nu}B^{\alpha\beta}B_{\alpha\beta}) \\ &+ \frac{\mu^2\omega}{4\pi}(\phi_\mu\phi_\nu - \frac{1}{2}\phi_\alpha\phi^\alpha g_{\mu\nu}). \end{aligned} \quad (11)$$

In the weak field approximation we ignore higher order terms from the vector field in the energy momentum tensor. For the (0,0) component of the Ricci tensor we obtain

$$R_{00(1)} = -\frac{1}{2}\vec{\nabla}^2 h_{00}. \quad (12)$$

Substituting into equation (10) results in

$$-\frac{1}{2}\vec{\nabla}^2(h_{00}) = 4\pi G_0 \rho. \quad (13)$$

Varying the action with respect to ϕ^μ gives the field equation:

$$\nabla_\nu B^{\mu\nu} - \mu^2 \phi^\mu = -\frac{4\pi}{\omega} J^\mu. \quad (14)$$

Let us assume that the current, J^μ , is conserved: $\nabla_\mu J^\mu = 0$ (For constant κ , this is equivalent to conservation of the matter current ρu^μ). In the weak field approximation this implies the constraint $\phi^\mu_{,\mu} = 0$ which, for the static case, simplifies to

$$\vec{\nabla}^2 \phi^0 - \mu^2 \phi^0 = -\frac{4\pi}{\omega} J^0. \quad (15)$$

This has the solution of

$$\phi^0(x) = \frac{1}{\omega} \int \frac{e^{-\mu|\vec{x}-\vec{x}'|}}{|\vec{x}-\vec{x}'|} J^0(\vec{x}') d^3 x'. \quad (16)$$

Taking the divergence of the test particle equation of motion (6), applying the weak field approximation, and ignoring time derivatives gives

$$\vec{\nabla} \cdot \mathbf{a} - \frac{1}{2}\vec{\nabla}^2 h_{00} = -\omega\kappa\vec{\nabla}^2 \phi^0, \quad (17)$$

where "a" represents the acceleration of the test particle. We define an effective potential, which determines the test particle acceleration, by $\mathbf{a} = -\vec{\nabla}\Phi_{eff}$. Substituting $\vec{\nabla}^2 h_{00}$

from (13) into (17) relates Φ_{eff} to the distribution of matter:

$$\vec{\nabla} \cdot (\vec{\nabla}\Phi_{eff} - \kappa\omega\vec{\nabla}\phi^0) = 4\pi G_0 \rho. \quad (18)$$

Inserting ϕ^0 from (16), and setting $J^0 = \kappa\omega\rho$, gives the effective potential due to a mass distribution $\rho(\vec{x})$:

$$\Phi_{eff}(\vec{x}) = -\int \frac{G_0\rho(\vec{x}')}{|\vec{x}-\vec{x}'|} d^3 x' + \kappa^2 \int \frac{e^{-\mu|\vec{x}-\vec{x}'|}}{|\vec{x}-\vec{x}'|} \rho(\vec{x}') d^3 x'. \quad (19)$$

Setting $\kappa = \sqrt{\alpha G_N}$ and $G_0 = (1+\alpha)G_N$ gives the conventional form derived in Moffat & Rahvar (2013)

$$\Phi_{eff}(\vec{x}) = -G_N \left[\int \frac{\rho(\vec{x}')}{|\vec{x}-\vec{x}'|} (1+\alpha - \alpha e^{-\mu|\vec{x}-\vec{x}'|}) d^3 x' \right]. \quad (20)$$

Consequently, the acceleration of a test particle is given by

$$\begin{aligned} \mathbf{a}(\mathbf{x}) &= -G \int \frac{\rho(\mathbf{x}')(\mathbf{x}-\mathbf{x}')}{|\mathbf{x}-\mathbf{x}'|^3} \\ &\times \left[1 + \alpha - \alpha e^{-\mu|\mathbf{x}-\mathbf{x}'|} (1 + \mu|\mathbf{x}-\mathbf{x}'|) \right] d^3 x' \end{aligned} \quad (21)$$

Using this theory to analyze observations of spiral galaxies and clusters of galaxies yields the unique values, $\alpha = 8.89 \pm 0.34$ and $\mu = 0.04 \pm 0.004 \text{ kpc}^{-1}$, that fit with the spiral galaxies and cluster of galaxies (Moffat & Rahvar 2013, 2014).

2.2 Non-Local Gravity

Lorentz covariance in special relativity is valid for inertial observers. The fundamental assumption of transformation of physical laws between non-accelerating observers and accelerating observers is that, locally, these two frames are equivalent. This is called the equivalence principle. However, for accelerating observers who are real observers of the physical world, Lorentz covariance might not be valid. This extension is modelled with the introduction of non-locality in the accelerating frames and consequently in gravity.

It has been argued that one must in general go beyond the locality hypothesis of standard special relativity theory and include the past history of an accelerated observer (Mashhoon 1993). The extension of non-locality to general relativity is done by an averaging procedure where a kernel acts as the weight function for the gravitational memory of the past events. In Non-Local Gravity, it is assumed that deviation from locality is proportional to λ/\mathcal{L} where λ is the characteristic length of phenomena and \mathcal{L} is a characteristic length determined by the acceleration of the observer. In the case that $\lambda/\mathcal{L} > 1$, assuming that the locality is broken, we cannot use the equivalence principle.

Non-Local Gravity is formulated in a tetrad formalism. The tetrad field relates the space time metric to a local Minkowski frame through $g_{\mu\nu}(x) = e_\mu^{\hat{\alpha}} e_\nu^{\hat{\beta}} \eta_{\hat{\alpha}\hat{\beta}}$. Here the tetrad field has sixteen degrees of freedom. It is necessary to extend the Riemannian structure of space-time by using the Weitzenböck connection where $\nabla_\mu e^{\hat{\alpha}}{}_\nu = 0$. Simplifying this equation results in $\Gamma^\lambda{}_{\mu\nu} = e^\lambda{}_{\hat{\alpha}} \partial_\mu e^{\hat{\alpha}}{}_\nu$.

Similar to the electromagnetic field (Blagojević & Hehl

2012; Aldrovandi & Pereira 2013; Maluf 2013), we can define the field strength as follows

$$C_{\mu\nu}^{\hat{\alpha}} = \partial_{\mu} e_{\nu}^{\hat{\alpha}} - \partial_{\nu} e_{\mu}^{\hat{\alpha}}. \quad (22)$$

We define another auxiliary field, a modified torsion tensor:

$$\mathfrak{C}_{\mu\nu}^{\hat{\alpha}} = \frac{1}{2} C_{\mu\nu}^{\hat{\alpha}} - C_{[\mu\nu]}^{\hat{\alpha}} + 2e_{[\mu}^{\hat{\alpha}} C_{\nu]}^{\hat{\beta}}. \quad (23)$$

By defining the tensor density

$$\mathcal{H}^{\mu\nu}{}_{\rho}(x) = \frac{\sqrt{-g(x)}}{\kappa} \mathfrak{C}^{\mu\nu}{}_{\rho}, \quad (24)$$

with $\kappa = 8\pi G$, the Einstein equation can be written in the simpler form:

$$\partial_{[\mu} C_{\nu\rho]}^{\hat{\alpha}} = 0, \quad (25)$$

$$\partial_{\nu} \mathcal{H}^{\mu\nu}{}_{\hat{\alpha}} = \sqrt{-g} (T_{\hat{\alpha}}{}^{\mu} + E_{\hat{\alpha}}{}^{\mu}), \quad (26)$$

where $T_{\hat{\alpha}}{}^{\mu}$ is the energy-momentum tensor of matter and $E_{\hat{\alpha}}{}^{\mu}$ is the energy-momentum of the tetrad field. Similar to the energy-momentum tensor of electromagnetic field, the latter is traceless. The advantage of teleparallel formalism of general relativity is that we can write the Einstein equations in the form of Maxwell equations in non-vacuum media. Here $C_{\mu\nu}^{\hat{\alpha}}$ plays a role similar to the electromagnetic field tensor $F_{\mu\nu}$ (i.e. $C_{\mu\nu}^{\hat{\alpha}} \rightarrow F_{\mu\nu}$), $\mathcal{H}^{\mu\nu}{}_{\hat{\alpha}}$ plays the role of displacement tensor of $H_{\mu\nu}$ (i.e. $\mathcal{H}^{\mu\nu}{}_{\hat{\alpha}} \rightarrow H_{\mu\nu}$) and finally $\sqrt{-g} (T_{\hat{\alpha}}{}^{\mu} + E_{\hat{\alpha}}{}^{\mu})$ plays the role of current in the electromagnetism (i.e. $\sqrt{-g} (T_{\hat{\alpha}}{}^{\mu} + E_{\hat{\alpha}}{}^{\mu}) \rightarrow j^{\mu}$).

It is well known that the constitutive relation between $F_{\mu\nu}$ and $H_{\mu\nu}$ in the electrodynamics of a generic medium is non-local. This non-locality is expressed through a kernel in the integration. This idea is extended to non-local relativity in a covariant form. In the weak field approximation, by expanding the tetrad field around $\delta^{\alpha}{}_{\mu}$, equation (26) can be written as (Rahvar & Mashhoon 2014)

$$\frac{\partial}{\partial x^{\sigma}} \left[\mathfrak{C}_{\mu}{}^{\sigma}{}_{\nu}(x) + \int \mathcal{K}(x, y) \mathfrak{C}_{\mu}{}^{\sigma}{}_{\nu}(y) d^4 y \right] = \kappa T_{\mu\nu}. \quad (27)$$

The (0, 0) component of this equation reduces to the modified Poisson equation

$$\nabla^2 \phi = 4\pi G(\rho + \rho_D), \quad (28)$$

where ϕ represents the gravitational potential and is related to the test particle acceleration by $d^2 x/dt^2 = -\nabla\phi$. Here ρ_D is an extra term in the Poisson equation that resembles dark matter, but that arose entirely from the effects of non-local gravity. It is given by

$$\rho_D(x) = \int q(|x - y|) \rho(y) d^3 y, \quad (29)$$

where $q(|x - y|)$ is the kernel of non-locality. We adapt the kernel

$$q = \frac{1}{4\pi\lambda_0} \frac{(1 + \mu r)}{r^2} e^{-\mu r}. \quad (30)$$

where μ is a constant with dimension of inverse length, and λ_0 is the fundamental length scale of NLG which may depend on the size of structure. Here we assume λ_0 is a constant parameter. By introducing a dimensionless parameter α we can write $\lambda_0 = \frac{2}{\mu\alpha}$.

Substituting this kernel in the definition of the potential, and integrating, we obtain the acceleration of a test particle:

$$\begin{aligned} \mathbf{a}(\mathbf{x}) &= -G \int \frac{\rho(\mathbf{x}')(\mathbf{x} - \mathbf{x}')}{|\mathbf{x} - \mathbf{x}'|^3} \\ &\times \left[1 + \alpha - \alpha e^{-\mu|\mathbf{x} - \mathbf{x}'|} \left(1 + \frac{\mu}{2} |\mathbf{x} - \mathbf{x}'| \right) \right] d^3 x' \end{aligned} \quad (31)$$

Comparing this acceleration with equation (21) for MOG, the only difference between these two theories is an extra factor of 1/2 in the second term.

A more general situation can be supposed if we use one of the following kernels:

$$q_1 = \frac{1}{4\pi\lambda_0} \frac{1 + \mu(a_0 + r)}{(a_0 + r)^2} e^{-\mu r}, \quad (32)$$

$$q_2 = \frac{1}{4\pi\lambda_0} \frac{1 + \mu(a_0 + r)}{r(a_0 + r)} e^{-\mu r}, \quad (33)$$

which lead to the following acceleration law for non-local gravity:

$$\begin{aligned} \mathbf{a}(\mathbf{x}) &= -G \int \frac{\rho(\mathbf{x}')(\mathbf{x} - \mathbf{x}')}{|\mathbf{x} - \mathbf{x}'|^3} \\ &\times \left[1 - \mathcal{E}(r) + \alpha - \alpha e^{-\mu|\mathbf{x} - \mathbf{x}'|} \left(1 + \frac{\mu}{2} |\mathbf{x} - \mathbf{x}'| \right) \right] d^3 x'. \end{aligned}$$

Here $\mathcal{E}(r)$ is either $\mathcal{E}_1(r)$ or $\mathcal{E}_2(r)$ associated, respectively, to q_1 and q_2 and given by

$$\mathcal{E}_1(r) = \frac{a_0}{\lambda_0} \left\{ -\frac{r}{r + a_0} e^{-\mu r} + 2e^{\mu a_0} \left[E_1(\mu a_0) - E_1(\mu a_0 + \mu r) \right] \right\} \quad (34)$$

and

$$\mathcal{E}_2(r) = \frac{a_0}{\lambda_0} e^{\mu a_0} \left[E_1(\mu a_0) - E_1(\mu a_0 + \mu r) \right], \quad (35)$$

where $E_1(u)$ is the exponential integral function:

$$E_1(u) := \int_u^{\infty} \frac{e^{-t}}{t} dt. \quad (36)$$

The best fitting parameter values for the simple kernel in equation (30), obtained by comparing the dynamics of spiral galaxies with the theory, are $\alpha = 10.94 \pm 2.56$ and $\mu = 0.059 \pm 0.028 kpc^{-1}$ (Rahvar & Mashhoon 2014).

2.3 Modified Newtonian Dynamics (MOND)

Another interesting alternative for addressing the missing mass problem is the Modified Newtonian Dynamics, proposed by Milgrom (1983). To explain the flat rotation curves of spiral galaxies, Milgrom assumed that Newtonian dynamics should be modified in a way that preserves Newtonian gravity at large accelerations but is modified at low accelerations. This theory introduces a universal acceleration $a_0 = 1.0 \times 10^{-10} \text{ m s}^{-2}$ below which the Newtonian dynamics is modified. An equivalent version of this theory is the modified gravitational acceleration g , sourced by a point mass M , as follows:

$$g = \begin{cases} GM/r^2 & g \gg a_0, \\ \sqrt{GMa_0}/r & g \ll a_0. \end{cases} \quad (37)$$

To obtain a smooth transition between the two regimes, between the Newtonian gravity and Mondian gravity, Milgrom's law is written in the following form:

$$g_N = \mu\left(\frac{g}{a_0}\right)g, \quad (38)$$

where the interpolating function μ satisfies: $\mu(x) \rightarrow 1$ for $x \gg 1$ and $\mu(x) \rightarrow x$ for $x \ll 1$. A standard choice for the interpolating function is:

$$\mu(x) = x(1+x^2)^{-1/2}. \quad (39)$$

From this interpolating function, it is straight forward to find the acceleration of a test particle, relative to the Newtonian acceleration, by using equations (38) and (39):

$$g = \frac{g_N}{\sqrt{2}} \sqrt{1 + \sqrt{1 + \left(\frac{2a_0}{g_N}\right)^2}}. \quad (40)$$

It has been known for years that MOND does not completely explain the mass discrepancy in galaxy clusters (Sanders 1999). However by using MOND the amount of estimated missing mass in clusters reduces significantly and roughly the unseen mass would be as much as observed baryonic mass. One candidate for this undetected mass is cosmological neutrinos with the mass of the order of $2eV$ (Sanders 2007; Angus et al. 2007).

3 ROTATION CURVES OF GALAXIES

In this section, we use so-called dwarf galaxies to test the three alternative gravity theories. Our aim is to explain the dynamics of structures, from the smallest galaxies to clusters of galaxies, without using the concept of dark matter. Dwarf galaxies are smaller than spiral galaxies. In dark matter models, some dwarf galaxies have a higher ratio of dark matter to baryonic matter compared to spiral galaxies (de Blok & McGaugh 1997).

Similar to the procedures used in Moffat & Rahvar (2013, 2014), we use the distribution of baryonic matter of dwarf galaxies, including stars and interstellar baryonic gas, to analyze the galaxy rotation curves. We assume, for simplicity, that galaxies have cylindrical symmetry. For both MOG and NLG the radial component of acceleration can be calculated by discretizing space into small elements and linear summing of the accelerations due to each element as follows:

$$a_r(r) = G_N \sum_{r'=0}^{\infty} \sum_{\theta'=0}^{2\pi} \frac{\Sigma(r')}{|r-r'|^3} (-r+r'\cos\theta')(1+\alpha - \alpha e^{-\mu|r-r'|} - \mu\alpha\beta|r-r'|e^{-\mu|r-r'|})r'\Delta r'\Delta\theta', \quad (41)$$

where β for MOG is 1 and for NLG is 1/2, and $\Sigma(r)$ represents the column density of the galaxy. In the case of MOND, since the theory is non-linear, we first find the Newtonian acceleration (i.e. g_N), as in standard Newtonian gravity, and then obtain the MOND acceleration according to equation (40).

From the observations, we have the surface Luminosity of stars, as well as the column density of gas. Here we choose a sub-sample of nearby galaxies from the LITTLE THINGS catalog with high resolution measurements (Hunter et.al 2015). Details about the observational parameters of these galaxies are given below.

3.1 LITTLE THINGS catalog

Local Irregulars That Trace Luminosity Extremes, The HI Nearby Galaxy Survey (LITTLE THINGS) is a high-resolution ($\sim 6''$ angular; $<2.6 \text{ km s}^{-1}$ velocity resolution) survey of nearby (within 10.3 Mpc) dwarf galaxies in the local volume observed with the Very Large Array (VLA). Galaxies with distances >10 Mpc have been excluded in order to achieve a reasonably small spatial resolution in VLA HI maps. The mean distance to the galaxies in the LITTLE THINGS sample is 3.7 Mpc. In addition galaxies with $W_{20} > 160 \text{ km s}^{-1}$ have been excluded in order to fit the galaxy emission comfortably in the bandwidth available for the desired velocity resolution (Oh et al. 2015). Here, W_{20} is the full-width at 20% of the peak of an integrated HI flux-velocity profile.

The high-resolution HI observations enable us to derive reliable rotation curves of the sample galaxies in a homogeneous and consistent manner. The rotation curves are then combined with the Spitzer archival $3.6 \mu\text{m}$ and ancillary optical U, B, and V images to construct mass models of the galaxies. Spitzer IRAC $3.6 \mu\text{m}$ images are less affected by dust and less sensitive to the young stellar populations compared with optical images, making them better for tracing old stellar populations found in dwarf galaxies. This high quality, multi-wavelength dataset significantly reduces observational uncertainties and thus allows us to examine in detail the mass distribution in the galaxies (Hunter et.al 2015). In high resolution HI data, observational systematic effects are properly reduced, which provides us more accurate data.

The LITTLE THINGS catalog contains 37 dwarf galaxies, but the rotation curve and the mass model of 26 dwarf galaxies are available (Hunter et.al 2015). For our analysis we choose a sub-sample of 16 dwarf galaxies for which the data has good coverage of rotation curves. Table (1) shows the list of galaxies in the sub-sample of the LITTLE THINGS catalog.

3.2 Comparing modified gravity models with the observations of Little Things galaxies

In this section we fit the three modified gravity models to the dynamics of dwarf galaxies in LITTLE THINGS catalog. We note that In the Newtonian gravity, one of crucial parameters in the estimation of dark matter content of a structure is the overall mass to the light ratio of a structure where we can extract the mass from the dynamics of structure and luminosity from the apparent luminosity of structure after correcting for absorption in the intergalactic and galactic media.

The luminosity of galaxies in our study is given in terms of magnitude in V-band (Hunter et al. 2012) and dynamics of galaxies are also obtained from the rotation curve of galaxies (Hunter et.al 2015).

3.2.1 Fitting observations with MOG

For the mass models of dwarf galaxies, we define a linear interpolation function to construct the mass profile from the centre to the edge of galaxy. In the observation we have the brightness of galaxies which has to be translated to

the mass profile. The observations for each galaxy give data points (x_i, F_i) , where x_i is the distance from the centre of the galaxy and F_i is the surface brightness at x_i . We define a continuous surface brightness profile $F(x)$ for stars by setting

$$F(x) = F_i + \frac{F_{i+1} - F_i}{x_{i+1} - x_i}(x - x_i), \quad (42)$$

And continuous column density profile for gas by setting

$$\Sigma^{gas}(x) = \Sigma_i^{gas} + \frac{\Sigma_{i+1}^{gas} - \Sigma_i^{gas}}{x_{i+1} - x_i}(x - x_i), \quad (43)$$

for x between x_i and x_{i+1} . The column density of each galaxy is given by $\Sigma = \Upsilon_*^{(3.6)} F + \Sigma^{gas}$. Using this continuous column density, and assuming universal values for the parameters μ and α , we can numerically compute the integral in equations (21) and (31) for a test particle at radial position of " x ". Moreover we do the same procedure using a universal value of $a_0 = 1.0 \times 10^{-10} \text{ m s}^{-2}$ in MOND and compute the equation (40). The radial acceleration provides the rotation curve of stars and gas, and consequently the overall rotational curve of the galaxies in MOG, NLG and MOND. Here we let the stellar mass to the light ratio in $3.6\mu\text{m}$ as the free parameter to fit the observation with the prediction of different models. The goodness of fit for each galaxy is calculated by χ^2 fit and the minimum value for this function provides the best $\Upsilon_*^{(3.6)}$ for each galaxy:

$$\chi^2 = \sum_{i=1}^N \frac{(V_i^{th} - V_i^{obs})^2}{\sigma_i^2}, \quad (44)$$

here σ_i is the uncertainty of V_i^{obs} and N is the number of data points. To see if MOG, NLG and MOND can fit the rotation curve of dwarf galaxies we fix $\alpha = 8.89 \pm 0.34$ and $\mu = 0.042 \pm 0.004 \text{ kpc}^{-1}$ for MOG, $\alpha = 10.94 \pm 2.56$ and $\mu = 0.059 \pm 0.028 \text{ kpc}^{-1}$ for NLG and $a_0 = 1.0 \times 10^{-10} \text{ m s}^{-2}$ for MOND and let $\Upsilon_*^{(3.6)}$ to changes as the free parameter. The best value of $\Upsilon_*^{(3.6)}$ for different galaxies are given in the table (1) and the average value for the best χ^2 for these gravity models are: $\overline{\chi^2}_{MOG} = 1.14$, $\overline{\chi^2}_{NLG} = 0.84$ and $\overline{\chi^2}_{MOND} = 1.99$ which are reasonable values for the χ^2 fitting.

The best value for the stellar mass to light ratio of dwarf galaxies are also given in table (1). We note that the best value for $\Upsilon_*^{(3.6)}$ is different in various gravity models. This parameter for the case of MOND has the average value of $\Upsilon_*^{(3.6)}(MOND) = 1.91$ and for MOG and NLG the corresponding values are $\Upsilon_*^{(3.6)}(MOG) = 11.37$ and $\Upsilon_*^{(3.6)}(NLG) = 6.91$. A large difference in the values of stellar mass to the light ratio in the dwarf galaxies is crucial point that can falsify the gravity models. A larger value of the stellar mass to light ratio of dwarf galaxies are also suggested in the other works as Swaters et al. (2011) and Haghi & Amiri (2016) which is larger than the standard model for the star formation models. Larger Υ_* for dwarf galaxies might results from the different history of star formation in the dwarf galaxies than Milky Way. Having a diffuse medium as the dwarf galaxies may produce small mass stars. Since the luminosity of stars depends on the mass as $L \propto M^\alpha$ (Kuiper 1938; Salaris & Cassisi 2005), population of small mass stars results in higher stellar mass to the light ratio. On the other hand having a larger mass budget for the heavy

mass stars produces stellar remnant and the result is a larger mass to the light ratio. This question might be resolved with the future observations of stellar populations in the dwarf galaxies.

4 CONCLUSIONS

To test MOG, Non-Local Gravity and MOND models as the alternative models for the dark matter, we compared the theoretical rotation curves predicted by these three gravity models with the observed data for sixteen dwarf galaxies in the LITTLE THINGS catalog. The gravitational acceleration due to a point source in the weak field limit of MOG and Non-Local Gravity involves two parameters: α determines the gravitational coupling strength via $G = G_N(1 + \alpha)$ and μ as the inverse of the characteristic length of the repulsive Yukawa force. At distances much greater than μ^{-1} , the repulsive term is negligible. For each of MOG and Non-Local Gravity, we fix the parameters of μ and α with the universal values that has been reported in (Moffat & Rahvar 2013; Rahvar & Mashhoon 2014) and analyze the rotation curve of dwarf galaxies, using Υ_* at $3.6\mu\text{m}$ as the only free parameter of model. The same procedure for MOND has been done like the other gravity models. We fixed $a_0 = 1.0 \times 10^{-10} \text{ m s}^{-2}$ as the universal value which is consistent with the value obtained previously by fitting to spiral galaxies (Sanders & McGaugh 2002).

For the two modified gravity models of MOG and NLG, the value of Υ_* in the dwarf galaxies is larger than the conventional value in the Milky Way while for MOND we obtain a compatible value with the spiral galaxies. The stellar mass to the light ratio is a function of stellar population inside a galaxy where for population with larger mass stars this parameter would be smaller and for small mass population of stars, that will be larger. For diffused mediums as the dwarf galaxies, the history of star formation might be different and produce small mass stars. The result would be a larger stellar mass to the light ratio. On the other hand the remnant of heavy stars also can produce a larger stellar mass to the light ratio. This phenomenon can be examined by direct observations of stellar populations in the dwarf galaxies. Future telescope may resolve stars in the nearby dwarf galaxies and can rule out either MOG/NLG models or MOND.

ACKNOWLEDGMENTS

We thank John Moffat and Martin Green for their useful comments and improving the text of paper. Also we thank referee for his/her useful comments for improving this work.

REFERENCES

- Akerib, D. S., Araujo, H. M., Bai, X., et al. 2014, Physical Review Letters, 112, 091303
Aldrovandi, R., & Pereira, J. G. 2013, Teleparallel Gravity: An Introduction, Fundamental Theories of Physics, Volume 173. ISBN 978-94-007-5142-2. Springer Science+Business Media Dordrecht, 2013,
Angloher, G., Bauer, M., Bavykina, I., et al. 2012, European Physical Journal C, 72, 1971

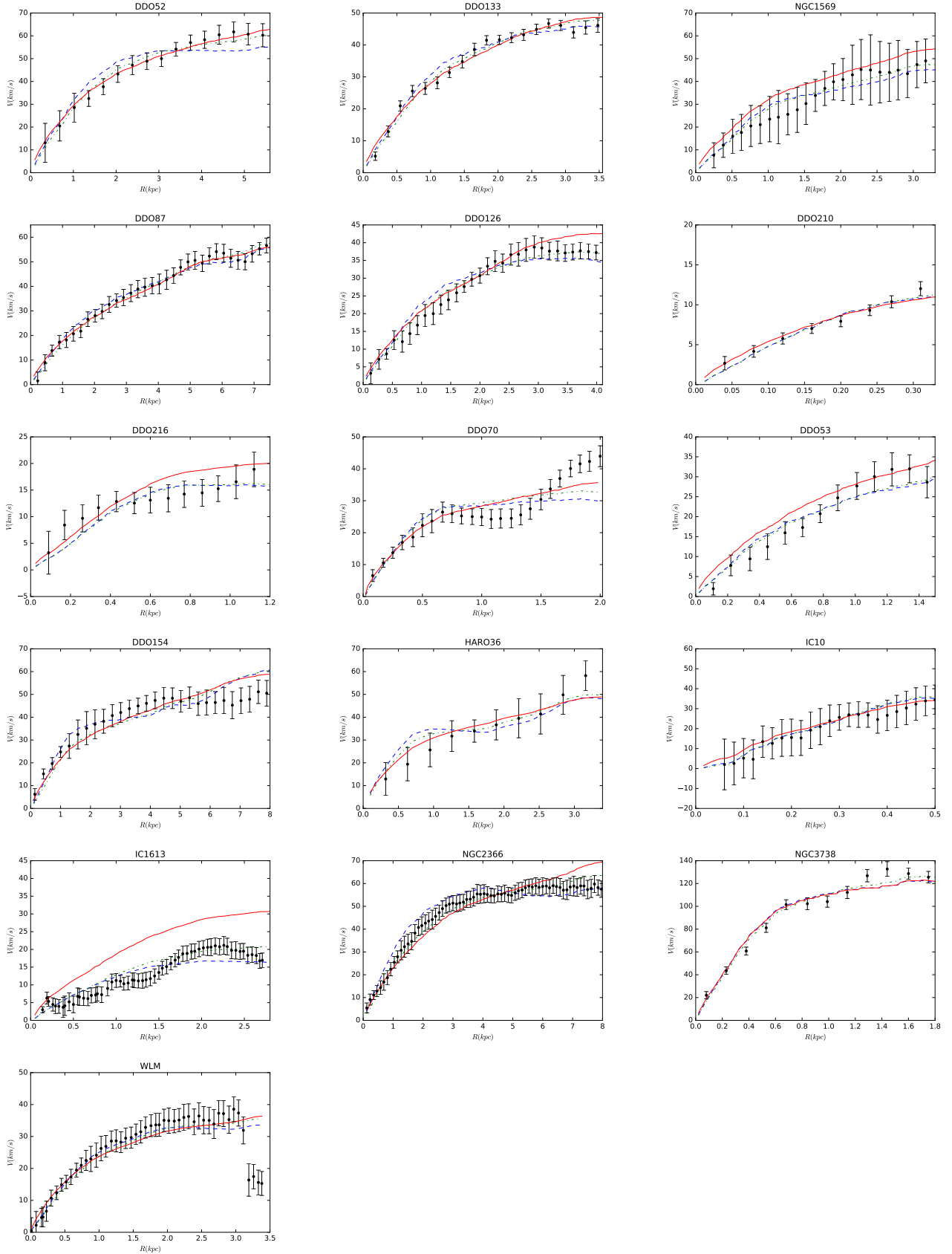


Figure 1. The best fits to the rotation velocity curves of the LITTLE THINGS sample. These curves are plotted using the universal value of $\alpha = 8.89 \pm 0.34$ and $\mu = 0.042 \pm 0.004 \text{ kpc}^{-1}$ (dashed line), $\alpha = 10.94 \pm 2.56$ and $\mu = 0.059 \pm 0.028 \text{ kpc}^{-1}$ (dashed-dotted line), and the rotation curve for MOND using the best value of $a_0 = 1.0 \times 10^{-10} \text{ m s}^{-2}$ (solid line).

Table 1. Sub-set of dwarf galaxies from THINGS catalog (Hunter et.al 2015), with fits to Modified Gravity. The columns are as follows: (1) name of the galaxy, (2) distance of the galaxy from us, (3) radius where the outermost part of the rotation curve is measured, (4) mass of gas, (5) stellar mass in 3.6 μm band, (6) normalized χ^2 for the best fit to the data in MOG, (7) normalized χ^2 for the best fit to the data in NLG, (8) normalized χ^2 for the best fit to the data in MOND, (9) best fit stellar mass to light ratio for MOG, (10) best fit stellar mass to light ratio for NLG, (11) best fit stellar mass to light ratio for MOND.

| Galaxy (1) | Distance (Mpc) (2) | R_{max} (kpc) (3) | M_{gas} ($10^{10}M_{\odot}$) (4) | M_{star} ($10^{10}M_{\odot}$) (5) | $\chi^2/N_{d.o.f}$ (MOG) (6) | $\chi^2/N_{d.o.f}$ (NLG) (7) | $\chi^2/N_{d.o.f}$ (MOND) (8) | $\Upsilon_{*MOG}^{(3.6)}$ M_{\odot}/L_{\odot} (9) | $\Upsilon_{*NLG}^{(3.6)}$ M_{\odot}/L_{\odot} (10) | $\Upsilon_{*MOND}^{(3.6)}$ M_{\odot}/L_{\odot} (11) |
|---------------|--------------------------|---------------------------|--|---|------------------------------------|------------------------------------|-------------------------------------|---|--|---|
| DDO 52 | 10.3 | 5.43 | 33.43 | 7.20 | 1.5 | 0.31 | 0.16 | $12.3^{+0.5}_{-0.6}$ | $6.5^{+0.3}_{-0.4}$ | $2.7^{+0.28}_{-0.26}$ |
| DDO 53 | 3.6 | 1.45 | 7.00 | 0.96 | 0.86 | 0.69 | 1.96 | $5.9^{+0.7}_{-0.7}$ | $4.1^{+0.7}_{-0.6}$ | $0.2^{+0.08}_{-0.08}$ |
| DDO 70 | 1.3 | 2.00 | 3.80 | 1.24 | 3.5 | 2.8 | 1.66 | $7.8^{+0.45}_{-0.40}$ | $5.9^{+0.2}_{-0.4}$ | $1.42^{+0.17}_{-0.2}$ |
| DDO 87 | 7.7 | 7.39 | 29.12 | 6.18 | 0.37 | 0.26 | 0.23 | $15.2^{+0.60}_{-0.45}$ | $6.8^{+0.28}_{-0.25}$ | $1.2^{+0.3}_{-0.1}$ |
| DDO 126 | 4.9 | 3.99 | 16.36 | 2.27 | 1.1 | 0.38 | 1.24 | $8.6^{+0.3}_{-0.4}$ | $4.6^{+0.24}_{-0.20}$ | $0.1^{+0.04}_{-0.04}$ |
| DDO 133 | 3.5 | 3.48 | 12.85 | 2.62 | 1.37 | 1.1 | 1.49 | $12.6^{+0.25}_{-0.40}$ | $7.6^{+0.2}_{-0.3}$ | $2^{+0.15}_{-0.15}$ |
| DDO 154 | 3.7 | 2.59 | 35.27 | 1.31 | 1.25 | 1.31 | 0.96 | $42.5^{+2.1}_{-2.0}$ | $19^{+1.2}_{-1.0}$ | $3.2^{+0.70}_{-0.65}$ |
| DDO 210 | 0.9 | 0.31 | 0.14 | 0.04 | 0.58 | 0.51 | 0.46 | $27.6^{+2.0}_{-1.9}$ | $24^{+1.8}_{-1.7}$ | $3.3^{+0.35}_{-0.54}$ |
| DDO 216 | 1.1 | 1.12 | 0.49 | 1.60 | 0.6 | 0.61 | 1.18 | $3.2^{+0.4}_{-0.4}$ | $2.6^{+0.35}_{-0.3}$ | $0.3^{+0.12}_{-0.12}$ |
| Haro36 | 9.3 | 3.16 | 11.16 | 5.81 | 0.62 | 0.37 | 0.35 | $8.0^{+1.2}_{-1.1}$ | $5.1^{+1.25}_{-1.2}$ | $1.4^{+0.51}_{-0.5}$ |
| IC 10 | 0.7 | 0.54 | 1.65 | 11.81 | 0.07 | 0.07 | 0.09 | $0.9^{+0.12}_{-0.14}$ | $0.8^{+0.08}_{-0.18}$ | $0.5^{+0.10}_{-0.12}$ |
| IC 1613 | 0.7 | 2.71 | 5.93 | 1.94 | 1.48 | 0.98 | 17.4 | $1.9^{+0.22}_{-0.13}$ | $1^{+0.05}_{-0.16}$ | $0.1^{+0.05}_{-0.05}$ |
| NGC 1569 | 3.4 | 3.05 | 20.24 | 20.69 | 0.16 | 0.1 | 0.45 | $1.89^{+0.25}_{-0.3}$ | $1.1^{+0.20}_{-0.20}$ | $0.5^{+0.038}_{-0.038}$ |
| NGC2366 | 3.4 | 8.08 | 108.24 | 10.81 | 2.1 | 1.35 | 1.8 | $7.8^{+0.13}_{-0.25}$ | $2.8^{+0.15}_{-0.07}$ | $0.3^{+0.15}_{-0.05}$ |
| NGC3738 | 4.9 | 1.75 | 12.58 | 12.48 | 0.92 | 0.49 | 1.69 | $11.6^{+0.37}_{-0.35}$ | $9^{+0.30}_{-0.25}$ | $11.2^{+0.35}_{-0.30}$ |
| WLM | 1.0 | 3.04 | 7.96 | 1.23 | 1.8 | 2.14 | 2.37 | $14.2^{+0.6}_{-0.5}$ | $9.6^{+0.38}_{-0.35}$ | $2.2^{+0.15}_{-0.25}$ |

Angus, G. W., Shan, H. Y., Zhao, H. S., & Famaey, B. 2007, ApJ, 654, L13
 Bekenstein, J. D. 2004, Phys Rev D, 70, 083509
 Bevington, P. R., & Robinson, D. K. 2003, Data reduction and error analysis for the physical sciences, 3rd ed., by Philip R. Bevington, and Keith D. Robinson. Boston, MA: McGraw-Hill, ISBN 0-07-247227-8, 2003.,
 Blagojević, M., & Hehl, F. W. 2012, arXiv:1210.3775
 Blumenthal, G. R., Faber, S. M., Primack, J. R., & Rees, M. J. 1984, Nature, 311, 517
 Bruneton, J.-P., Liberati, S., Sindoni, L., & Famaey, B. 2009, J. Cosmology Astropart. Phys., 3, 021
 de Blok, W. J. G., & McGaugh, S. S. 1997, 290, 533
 Eisenstein, D. J., Zehavi, I., Hogg, D. W., et al. 2005, ApJ, 633, 560
 Gaitskell, R. J. 2004, Annual Review of Nuclear and Particle Science, 54, 315
 Haghi, H., & Amiri, V. 2016, MNRAS, 463, 1944
 Hehl, F. W., & Mashhoon, B. 2009, Physics Letters B, 673, 279
 Hunter, D. A., Ficut-Vicas, D., Ashley, T., et al. 2012, 144, 134
 Hunter, A. et.al 2015, arXiv:1502.01281v1 [astro-ph.GA] 4 Feb 2015
 Khoury, J. 2015, Phys. Rev. D, 91, 024022
 Kuiper, G. P. 1938, ApJ, 88, 472
 Maluf, J. W. 2013, Ann Phys 525, 339.
 Markevitch, M., Gonzalez, A. H., Clowe, D., et al. 2004, ApJ, 606, 819
 Mashhoon, B. 1993, Phys Rev A, 47, 4498
 Mashhoon, B. 2007, Annalen der Physik, 519, 57
 McGaugh, S., Lelli, F., & Schombert, J. 2016, arXiv:1609.05917
 Milgrom, M. 1983, ApJ, 270, 365
 Moffat, J. W., 2006, JCAP, 3, 4
 Moffat, J. W., Toth, V. T. 2008, ApJ, 680, 1158

Moffat, J. W., Toth, V. T., 2009, Classical and Quantum Gravity 26 (8), 085002
 Moffat, J. W., & Rahvar, S. 2013, MNRAS, 436, 1439
 Moffat, J. W., & Rahvar, S. 2014, MNRAS, 441, 3724
 Moore, B., Calcaneo-Roldan, C., Stadel, J., et al. 2001, Phys. Rev. D, 64, 063508
 Oh, S.-H., Hunter, D. A., Brinks, E., et al. 2015, AJ, 149, 180
 Rahvar, S., & Mashhoon, B. 2014, Phys. Rev. D, 89, 104011
 Rahvar, S., & Mashhoon, B. 2014, Phys Rev D, 89, 104011
 Rubin, V. C., Burbidge, E. M., Burbidge, G. R., & Prendergast, K. H. 1965, ApJ, 141, 885
 Rubin V. C. & Ford, W. K., Jr. 1970, ApJ, 159, 379
 Salaris, M., & Cassisi, S. 2005, Evolution of Stars and Stellar Populations, by Maurizio Salaris, Santi Cassisi, pp. 400. ISBN 0-470-09220-3. Wiley-VCH, December 2005., 400
 Sanders, R. H. 1999, ApJ, 512, L23
 Sanders, R. H., & McGaugh, S. S. 2002, ARA&A, 40, 263
 Sanders, R. H., & Land, D. D. 2008, MNRAS, 389, 701
 Sanders, R. H. 2007, MNRAS, 380, 331
 Spergel, D. N. 2015, Science, 347, 1100
 Swaters, R. A., Sancisi, R., van Albada, T. S., & van der Hulst, J. M. 2011, ApJ, 729, 118
 Swaters, R. A., Sanders, R. H., & McGaugh, S. S. 2010, ApJ, 718, 380
 Zwicky, F. 1937, ApJ, 86, 217